Modeling of snow and ice melt at ETH Camp (West Greenland): A study of surface albedo

Filip Lefebre,[1,2] Hubert Gallée,[3,4] Jean-Pascal van Ypersele,[1] and Wouter Greuell[5]

[1] The objective of this paper is to present the validation over Greenland of a thermodynamic snow-ice model that was complemented with the snow metamorphism and albedo parameterizations of the Centre d'Etudes de la Neige (Grenoble, France) in order to make the surface albedo variable and interactive. Special attention is given to the surface albedo since it is the most important parameter in energy exchanges with the atmosphere for snow and ice melt. The development of an integrated (snow, ice, and water) albedo model takes into account the different surface types observed on an ice sheet, and the snow albedo is calculated from the simulated surface snow grains. The validation for a polar site has been done at ETH Camp (West Greenland, 1155 m above sea level) during the 1990 and 1991 summer seasons. Although both ablation seasons differed greatly (in 1990 it showed a negative mass balance while in 1991 it ended with a positive mass balance), a single model configuration was able to provide good results for both 1990 and 1991. These simulations show that the snow metamorphism laws included enable an accurate simulation of the surface albedo and henceforth of the surface mass balance for a polar site, provided that the snow model is correctly forced at its surface level and that meltwater retention, percolation, and drainage are well represented in the snow model. The model results are also compared with two other modeling approaches, and differences between the three snow models are detailed. *INDEX TERMS:* 1827 Hydrology: Glaciology (1863); 1863 Hydrology: Snow and ice (1827); 3322 Meteorology and Atmospheric Dynamics: Land/atmosphere interactions; 3349 Meteorology and Atmospheric Dynamics: Polar meteorology; *KEYWORDS:* modeling surface albedo on Greenland, snow albedo, modeling surface mass balance at ETH Camp, Greenland surface mass balance

1. Introduction

[2] The consequences of a future climate change will be most important for the polar regions due to the positive snow and ice albedo feedback mechanism. Long-term global model simulations that are currently carried out to assess the consequences of an observed, and still continuing, CO_2-concentration increase are based on numerous parameterizations. Globally-averaged model sensitivity to a CO_2-doubling ranges from 1.5 to 4.5 degrees Celsius at equilibrium [*Houghton et al.*, 2001]. This is partly due to different sub-grid parameterizations (e.g., for cloud, radiation, precipitation and turbulence) used in the various climate models.

[3] Besides uncertainties related to the atmospheric part of the models, other difficulties arise from the representation of the polar snow and ice surfaces. To emphasize the importance of snow cover parameterizations in climate models, *Randall et al.* [1994] examined the snow-temperature feedback in 14 global circulation models (GCMs). Not only positive but also negative feedbacks were found due to the large variety of parameterizations. Especially, the albedo parameterization varied greatly.

[4] If we focus on Greenland, the diversity of the glaciological zones between the ice sheet margin ablation zone and the central dry snow zone [*Benson*, 1962] is not properly resolved in global climate models due to their rather coarse resolution. A way to look in detail at what happens on smaller scales is to use a regional atmospheric climate model (RaCM) forced at its boundaries with validated large-scale fields, i.e., nesting a RaCM into a GCM. If accurate surface mass balance estimates of Greenland are to be made with long-term climate simulations, the RaCM should contain a snow and ice sub-surface model and the surface albedo and roughness lengths should be correctly prescribed or simulated by the model. In this study we will

[1]Institut d'Astronomie et de Géophysique G. Lemaître, Université catholique de Louvain, Louvain-la-Neuve, Belgium.
[2]Now at Centre for Remote Sensing and Atmospheric Processes, Flemish Institute for Technological Research (VITO), Mol, Belgium.
[3]Laboratoire d'Étude des Transferts en Hydrologie et Environnement, Institut de Recherches pour le Développement, Grenoble, France.
[4]Now at Laboratoire de Glaciologie et Géophysique de l'Environnement, Saint-Martin d'Hères, France.
[5]Institute for Marine and Atmospheric Research, Utrecht University, Utrecht, Netherlands.

focus on the surface albedo modeling. The surface roughness length will not be examined although it is an important parameter in the surface layer turbulent flux calculations over melting surfaces [*Andreas*, 1987; *Munro*, 1989; *Smeets et al.*, 1999]. In high-latitude polar regions, a small variation in albedo will lead to a large difference in the absorbed solar energy, due to the intense solar radiation fluxes in summer. Therefore, a correctly modeled surface albedo is essential if surface mass balance calculations are to be carried out.

[5] *Gallée et al.* [1995] have validated "MAR" (Modèle Atmosphérique Régional), a mesoscale regional atmospheric model, for 2 days (12–13 July 1991) of the Greenland Ice Margin Experiment GIMEX [*Oerlemans and Vugts*, 1993]. The simple force-restore surface model of *Deardorff* [1978] was used to represent the ice sheet surface, which was acceptable for the short duration of the simulation. The surface model is called "force-restore" since the forcing induced by all surface fluxes is modified by a restoring term which contains the deep soil temperature. *Gallée and Duynkerke* [1997] completed a three-week (5–24 July 1991) two-dimensional simulation for the GIMEX transect with MAR coupled to a multi-layered thermodynamic snow-ice model with a prescribed surface albedo. Taking into account the "refreezing of internal meltwater" significantly improved the simulation.

[6] Recently, the snow-ice model has been improved by adding the snow metamorphism and snow albedo laws of the CEN (Centre d'Etudes de la Neige) snow model CROCUS [*Brun et al.*, 1992] in order to make the surface albedo completely interactive. In this new model version, snow albedo is calculated from the simulated surface snow grains. Moreover, an integrated albedo model has been developed that takes into account the presence of snow, ice and water at the surface. This improved version of the snow-ice model has been tested for the winter of 1993–1994 at the Col de Porte in the French Alps, which proved the compatibility of the former version of the model with the CROCUS snow metamorphism laws [*Gallée et al.*, 2001]. However, CROCUS snow metamorphism laws have been initially developed and tested for snow covers in mid-latitude Alpine regions so it appears necessary to test and validate the improved snow-ice model for a polar site on Greenland before it is ready to be used in coupled atmosphere-snow regional climate simulations. *Dang et al.* [1997] have shown that CROCUS is able to reproduce the major features of the snow cover at the South Pole, but meteorological and glaciological conditions at the South Pole differ greatly from those prevailing in the ablation zone of the Greenland ice sheet where the snow cover, which lies upon an almost impermeable ice surface, melts during the summer. Moreover, the small surface slope enables meltwater to accumulate and a slush layer can develop during the summer melt season.

[7] In the present paper, the snow-ice model alone, forced at its surface with measurements, will be used for the ablation seasons 1990 and 1991 at ETH Camp (West Greenland, 1155 m above sea level (asl), see Figure 1).

[8] ETH Camp is an ideal location for testing a snow-ice model during an ablation season in Greenland as it is close to the long-term equilibrium line where many snow-ice processes such as retention, percolation, refreezing and runoff of meltwater, are involved. The two summers for which the model will be tested differ greatly and represent
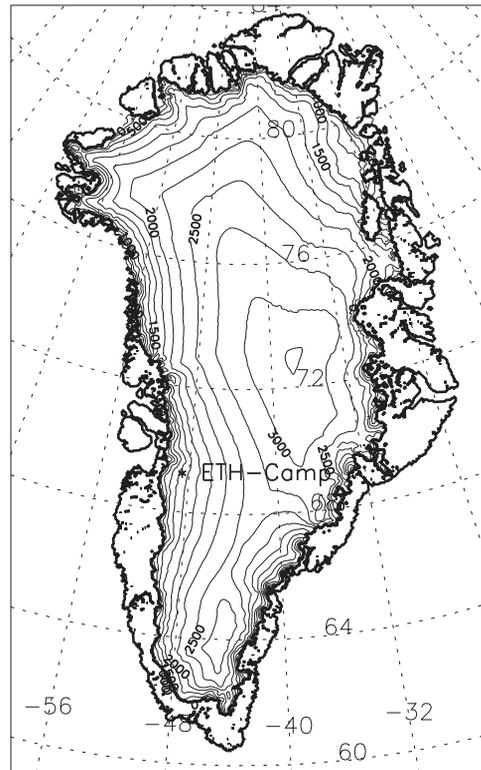

Figure 1. Map of Greenland. The location of ETH Camp is marked with a star.

consequently a more severe test than a one-season simulation. The duration of the two simulations equals 79 and 77 days for the 1990 and 1991 seasons, respectively. As mentioned above, focus will be on the surface albedo behavior which is one of the most important uncertainties still remaining in snow melt models and snow cover parameterizations. During the two melting seasons at ETH Camp, the daily measured albedo (ratio of the total daily reflected radiation and the total daily global radiation) fluctuated between 0.6 and 0.9 (with a mean of 0.707 and 0.770 for the duration of the 1990 and 1991 simulations, respectively) and we are examining the extent to which the incorporated snow metamorphism and snow albedo laws can capture these variations, quantitatively and qualitatively.

2. Snow-Ice Model Description

[9] The snow-ice model is part of the regional atmospheric climate model MAR [*Gallée*, 1995; *Marbaix*, 2000] as an interactive lower boundary. In MAR the snow-ice model feeds back to the atmosphere by means of surface temperature, specific humidity close to the surface, roughness lengths, and surface properties (albedo, emissivity). In the present study, it will be used in stand-alone configuration, i.e., the snow-ice model will be forced with measured atmospheric variables and radiation fluxes.

[10] The snow-ice model is a multi-layered one-dimensional model and consists of a thermodynamic module, a water balance module, a snow metamorphism and settling module, a snow cover discretization control module and an integrated surface albedo module. The one-dimensionality

of the snow-ice model is a valid hypothesis since a RaCM horizontal grid size is much larger than the vertical extension of the snow-ice model.

[11] The thermodynamic module solves the thermal diffusion equation. When snow or ice temperatures are above the melting point, temperature is put back to zero degrees and melting takes place. A fraction of the internal meltwater is retained inside the snow pack assuming a maximum value for the liquid water content [*Colbeck*, 1972] and meltwater can accumulate above ice or snow layers having high densities or saturated by liquid water. A complete description of the thermodynamic and water balance modules is given by *Gallée and Duynkerke* [1997]. A key-parameter in the water retention and percolation treatment is the snow layer maximum water content (maximum water saturation, irreducible water saturation). Different values can be found in the literature [*Rowe et al.*, 1995; *Greuell and Konzelmann*, 1994; *Denoth et al.*, 1979; *Brun*, 1989], generally between 0.02 and 0.1. Cold laboratory experimental results from *Coléou and Lesaffre* [1998] showed that the irreducible water saturation varies from 0.065 to 0.085 for homogeneous wet snow samples. A value of 0.07 has been chosen which is also the value suggested by *Colbeck* [1974]. The runoff of excessive internal and accumulated surface meltwater is based on the work of *Zuo and Oerlemans* [1996]. They proposed an algorithm for runoff of meltwater on ice at the GIMEX transect, which is situated 200 km south of ETH Camp. The rate of runoff is a function of three constants (c_1, c_2, c_3) and the surface slope (= S):

$$\frac{dW_r}{dt}\Big|_{runoff} = -\frac{W_r}{t^*} \tag{1}$$

where W_r is the surface water height or the internal liquid water content in excess of the maximum water saturation and $t^* = c_1 + c_2^* \exp(-c_3^* S)$ with S equal to the observed surface slope value (=0.02). c_1, c_2 and c_3 are set to 0.33 day, 25 days and 140, respectively. The value of c_1 differs from the one proposed by *Zuo and Oerlemans* [1996] (1 day). *Zuo and Oerlemans* [1996] only considered runoff of meltwater on ice. In our case, it is also used to drain excessive meltwater inside the snow pack. Therefore we prefer to use a smaller value for c_1 in order to evacuate more rapidly the excess meltwater in the snowpack. This rapid evacuation is due to the presence of vertical drainage channels and inhomogeneities at ETH Camp, which are described by *Konzelmann* [1994].

[12] The ensemble of snow metamorphism parameterizations are taken from the CEN snow model CROCUS that were derived from cold laboratory experiments on natural snow samples. *Brun et al.* [1992] introduced a new formalism to describe the snow as a function of the continuous parameters such as temperature gradients and liquid water content of the snow pack. The snow grain parameters in the new formalism are dendricity, sphericity and descriptive grain size. Here we will only discuss the main characteristics of this formalism.

[13] Fresh snow (called dendritic snow) is described by its dendricity and sphericity. Dendricity always decreases from 1 for fresh dendritic-shaped crystals to 0. It describes the part of the original crystal shapes which are still remaining in a snow layer. Sphericity describes the ratio

of rounded versus angular shapes. The prescribed dendricity and sphericity of freshly fallen snow mainly depends on the intensity of the surface wind. The dendritic snow grains evolve rapidly through disintegration and combined sublimation-deposition processes which also tend to dissipate the smaller particles in favor of bigger ones. When dendricity becomes equal to 0, the snow grains arrive at the stage of rounded (sphericity = 1) crystals, faceted (sphericity = 0) crystals or at an intermediate state depending on the temperature gradients that were present in the snow pack. The snow grains are now called nondendritic snow grains and are characterized by their sphericity and their descriptive grain size. Sphericity again describes the ratio of rounded versus angular shapes while the descriptive grain size indicates the average size of the snow crystals.

[14] An integrated surface albedo model has been developed that takes into account not only the presence of snow at the surface but also of ice and accumulated meltwater. If snow depth (defined as the thickness of the snow pack above last year's "old" ice or this year's "new" superimposed ice) becomes less than 10 cm in melting conditions, a linear function is used to make a smooth transition between the snow and ice ($\alpha = 0.58$) albedo. The value of the ice albedo is representative for the ice albedo values encountered at ETH Camp and is taken from *Greuell and Konzelmann* [1994]. If snow depth is zero, surface albedo varies exponentially between the ice ($\alpha = 0.58$) and water ($\alpha = 0.15$) albedo as a function of the accumulated surface water height. If snow depth is greater than 10 cm, surface albedo equals the snow albedo which is calculated with the albedo-parameterizations of the CROCUS snow model [*Brun et al.*, 1992]:

$$\alpha_{(0.3-0.8\mu m)} = 1 - 1.58(d)^{1/2} \tag{2}$$

$$\alpha_{(0.8-1.5\mu m)} = 1 - 15.4(d)^{1/2} \tag{3}$$

$$\alpha_{(1.5-2.8\mu m)} = 346.3d - 32.31(d)^{1/2} + 0.88 \tag{4}$$

where d is the optical grain size expressed in m. The optical grain size is also calculated with parameterizations of the CROCUS snow model [*Brun et al.*, 1992]. It corresponds to the size of the spherical grains of a theoretical snow sample whose computed albedo equals the albedo of the considered snow.

[15] When the snow-ice model is coupled to an atmospheric model with sophisticated solar radiation transfer functions, the simulated solar radiation spectrum should be split into the three spectral intervals of equations (2), (3) and (4). This should be done since clouds modify the spectral composition of the solar light distribution [*Wiscombe and Warren*, 1980]. In the present case, no spectral information was available; a prescribed solar light distribution is used (0.606, 0.301 and 0.093 are the fractions for the three spectral intervals of $0.3-0.8$ μm, $0.8-1.5$ μm and $1.5-2.8$ μm, respectively) [*Coulson*, 1975]. A sensitivity experiment with a distribution used in CROCUS (0.590, 0.310, 0.100 for the three spectral intervals, respectively) revealed no important sensitivity. In the future, coupling of the atmosphere and snow model will make this prescription of the solar radiation distribution redundant.
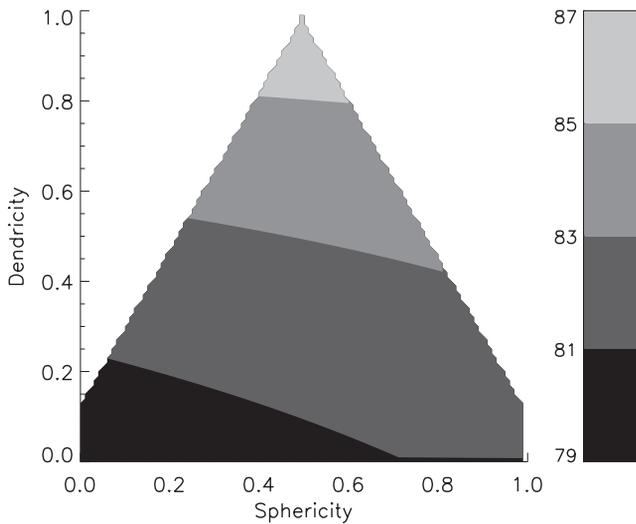
Figure 2. Snow albedo for dendritic snow calculated with CROCUS snow metamorphism laws.

[16] Freshly fallen dendritic snow (sphericity = 0.5, dendricity = 1.0, see Figure 2) has a high ($\alpha = 0.87$) albedo because its optical grain size lies between 0.1 and 0.2 mm. The breaking of the branched ice crystals lowers the dendricity and albedo falls to a value of 0.79.

[17] The albedo of nondendritic snow decreases as the snow grains become larger (see Figure 3). The reason for the higher albedo values of faceted crystals compared to spherical crystals with the same descriptive grain size, lies in the calculation of the optical grain size for both types of snow grains. In the case of spherical snow grains, the optical grain size equals the descriptive grain size while in the case of faceted crystals, the optical grain size only corresponds to half the descriptive grain size, which leads to higher albedo values.

[18] Finally, the albedo-value (α_0) is further corrected by taking into account the solar zenith angle dependency according to *Segal et al.* [1991]:

$$\alpha = \alpha_0 + \max\left\{0; 0.32 * \frac{1}{2}\left[\frac{3}{1 + 4\cos\theta_z} - 1\right]\right\} \quad (5)$$

$$\cos\theta_z = \max(\cos 80°, \cos\theta_z) \quad (6)$$

where θ_z equals the solar zenith angle. Note that if the zenith angle is less than 60°, no correction is applied.

[19] The snow albedo aerosol and carbon soot content dependency should ideally also be included in the integrated surface albedo model, but it is acceptable to neglect this in our case as ETH Camp is located approximately at the equilibrium-line, i.e., some 40 km away from the ice sheet border.

[20] Fresh snow layers are derived from snowfall data at ETH Camp. A fresh snow layer is added to the snow pack when enough snow is available, i.e., when a fresh snow layer has a minimum thickness of 2 mm w.e. (water equivalent). The CROCUS parameterizations are used to determine the density, dendricity and sphericity of a fresh snow layer. In the case of snowfall events with a thickness of less than 2 mm w.e., the snowfall is not added directly to the snow model to keep the model numerically stable. However, the snow albedo is re-calculated from the fresh snowfall characteristics because tiny freshly fallen snow layers can change the surface albedo significantly. In order to preserve mass, the small snowfall is added to the next snowfall.

[21] The total number of snow and ice layers may change during the simulation. The snow grid has a maximum of 20 snow layers and the splitting or aggregation of snow layers is controlled by the CROCUS snow metamorphism laws in a way that preserves the natural stratigraphy of the snow pack. When an internal snow layer becomes thinner than 5 mm, it is aggregated with the snow layer below.

[22] Ice lenses within the snow pack are an often encountered phenomenon on the Greenland ice sheet due to refreezing of meltwater. In the present snow-ice model they are only poorly represented as they are treated as imperme-able, even though dye percolation studies have shown that these ice layers accelerate meltwater runoff [*Male*, 1980].

[23] Lastly, the calculation of the turbulent energy fluxes between the snow pack surface and the overlying atmos-phere is based on *Businger* [1973] formulations with a linear relationship for the momentum and heat stability functions ϕ_m and ϕ_h:

$$\phi_m = 1 + \alpha_m \frac{z}{L} \quad (7)$$

$$\phi_h = Pr + \alpha_h \frac{z}{L} \quad (8)$$

where $L = (u_*^2\,\theta)/(\kappa g \theta_*)$. u_*, θ, θ_*, and κ are equal to the friction velocity, the potential temperature, the turbulent temperature scale and the von Karman constant, respec-tively. We use a value of 6 for both α_m and α_h and a near-neutral turbulent Prandl number (Pr) of 1. This scheme is based on Monin-Obukhov's surface layer similarity theory [*Monin and Obukhov*, 1954]. Mass is removed from the highest snow layer in the case of sublimation. The roughness length for momentum (z_0) depends on the state
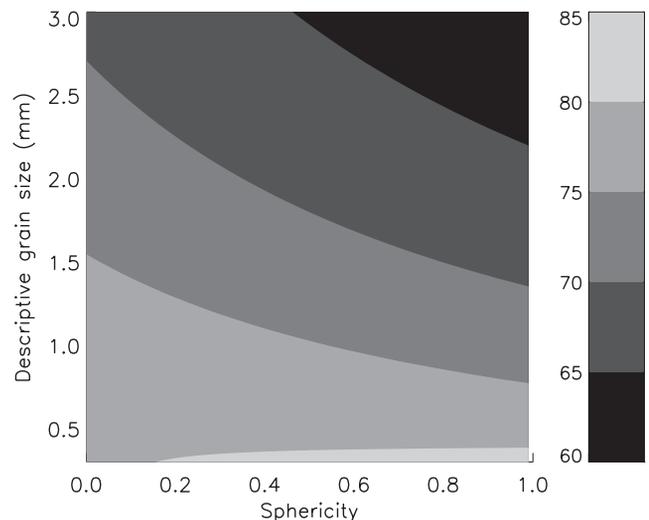

Figure 3. As in Figure 2, but for nondendritic snow.

Table 1. Snow Model Parameters Used in the Simulations

Parameter	Value
Snow layer maximum water content	0.07
Slope[a]	0.02
c_1, c_2, c_3[a]	1/3 day, 25 days, 140
Heat capacity of the snow	2105 $Jkg^{-1} K^{-1}$
Surface IR emissivity	1.00
Conductivity of pure ice	2.1 $Wm^{-1} K^{-1}$
Maximum number of snow layers	20
Number of ice layers	15
Minimum new snow layer thickness	2 mm w.e.

[a]Site-dependent parameters.

of the surface. In the model the same approach is used as that given by *Greuell and Konzelmann* [1994], who also modeled the 1990 melt season at ETH Camp. When the surface snow is not melting and has not been melting in the past, z_0 is set to 0.12 mm. In the case of surface melt, or if the surface snow has been melting in the past, z_0 is calculated from the surface snow or ice density [*Greuell and Konzelmann*, 1994]:

$$z_0 (\text{in mm}) = \max \left[1.3; 1.3 + (3.2 - 1.3) \frac{\rho_{\text{surf}} - 600}{920 - 600} \right] \quad (9)$$

where ρ_{surf} denotes the surface snow density in kg m^{-3}. This gives a value for z_0 between 1.3 and 3.2 mm.

[24] Although formulations are available to express the surface roughness length for heat and water vapor (z_h and z_q) as a function of z_0 and u_* [see, e.g., *Andreas*, 1987], the same approach as given by *Greuell and Konzelmann* [1994] has been used, i.e., z_h and z_q are taken equal to z_0.

[25] Sensitivity experiments in which the expressions of *Andreas* [1987] were used did not influence the results. This is due to the location of the site close to the equilibrium line, where sensible and latent heat fluxes tend to be of almost equal magnitude but opposite in sign (see section 3). The main snow model parameters are listed in Table 1.

3. Numerical Experiments

[26] The simulations consist of the one-dimensional snow-ice model forced at its surface by atmospheric measurements of the 1990 and 1991 ETH expeditions. Before presenting the results of the numerical experiments, some general characteristics of the two ETH expeditions are described. In spring 1990, the Swiss Federal Institute of Technology opened a campsite (69°34′25.3″ North, 49°17′44.1″ West, 1155 m above sea level) on the Greenland ice sheet to start an intensive measurement campaign during the 1990 ablation season [*Ohmura et al.*, 1991]. The following year, the campsite was re-opened and a second intensive measurement campaign was conducted [*Ohmura et al.*, 1992]. The location of the site is interesting because of the proximity of the long-term equilibrium line which is an indicator of climate change. The set-up of the two campaigns was almost identical. Wind, temperature and humidity sensors were mounted on a 30 m high tower (profile and turbulence measurements) and on the 10 m-high "synob"-mast. Solar and infrared fluxes, pressure and total precipitation supplement the atmospheric measurements. In 1991, the temperature and humidity sensors were

actively ventilated. In 1990, this was not the case so that during conditions of high global radiation and low wind speed a radiation error occurred.

[27] Surface and sub-surface measurements tracked the evolution of the snow and ice pack throughout the melting seasons. Thermistors provided temperature profiles down to a depth of 10 m. The average snow pack height and superimposed ice height were measured along stakes located in the "stake" area (at 0 and 12 UT) and information about density, liquid-water content and slush thickness were obtained from pits dug in the "pit" area (once a day at 18 UT). Since in 1990 the pits were dug inside the stake area, it is expected that in 1990 the pit measurements could have influenced the stake readings. In 1991, the pits were dug outside the stake area, not to disturb the stake observations. For the year 1990, the temperature, wind and humidity data come from the 30 m high tower, while for the 1991 experiments they come from the "synob"-mast.

[28] For a more complete description of the two ETH expeditions, the reader is referred to the two progress reports [*Ohmura et al.*, 1991, 1992], which give a detailed description of the climatological and environmental conditions encountered during the two melting seasons.

3.1. Case 1: Summer of 1990
3.1.1. Initialization of the Snow-Ice Model

[29] The initial state of the snow and ice pack is taken from the snow and ice measurements of the 12th of June 1990. The vertical extension of the model ice-grid equals 20 m. This large extension allows the assumption of a zero heat flux at the bottom of the model during the simulation.

[30] The height of the snow pack upon the ice is 1.14 m. Because no detailed layered snow density and liquid water content data could be obtained, the snow pack part of the snow-ice model has been initialized using the averaged reported snow density and liquid water content data although important gradients existed inside the snow pack. Average snow pack density equaled 396 kg m^{-3} with an average liquid water content of 1 volume %. Because on the 12th of June, the snow pack had already experienced 19 days of melt (the first signs of melt were observed on May 24th), the top 36 cm of the snow pack were initialized as wet and temperate snow. This was done in correspondence with the initial snow pack temperature profile on June 12th 1990 (see Figure 9.6 of *Ohmura et al.* [1991]).

[31] As with the snow density and liquid water content, no detailed information about the grain size profile is available. Therefore, we have set the model snow grains equal to those of typical dry and melting snow grains. The top 36 cm wet snow crystals have been characterized by spherical (sphericity = 1) grains with a size of 1.5 mm. The underlying dry snow crystals have been characterized by spherical 1.0 mm large snow crystals.

[32] *Konzelmann* [1994] also mentioned that at the beginning of the measurements, the snow cover already contained several ice lenses which cannot be taken into account during the initialization of the snow cover since ice lenses are only poorly represented in the snow-ice model.

3.1.2. Atmospheric Forcing Data

[33] The 1990 simulation begins the 12th of June and lasts until the 29th of August inclusive, i.e., 79 days. For

this period half-hourly measurements coming from the 30 m high tower (2 m temperature, 2 m specific humidity and wind at 10 m) and incoming short and long wave radiation as well as 6-hourly surface pressure and precipitation data have been processed in order to obtain the forcing data. The preparation was done as follows:

[34] 1. The measurements have been linearly interpolated in time down to the time step of the snow model (6 minutes). Missing data (2 days of solar and infrared incoming radiation data, 4 days of wind speed, temperature and specific humidity data) have been replaced by data from the "synob"-mast or through interpolation from data of an earlier and later day.

[35] 2. The measured specific humidity data has been corrected to allow for systematic errors. The calculated relative humidity never exceeded 90% during the observational period in spite of the occasional presence of fog. This leads us to assume a systematic error in the humidity measurements. Another argument supporting this is that the calculated average relative humidity (70%) does not correspond to the value of 79% reported by *Greuell and Konzelmann* [1994]. We have therefore multiplied the specific humidity by a factor of 1.1 in order to obtain saturation at some moments and to agree with the previously determined average relative humidity.

[36] 3. Wind speed measurements, taken at 10 m, have to be reduced to their value at 2 m by using the similarity laws in the nonneutral surface layer to be able to use the existing turbulence routine of MAR which supposes wind and temperature from the same height above the surface. In the surface-layer, wind speed at 2 m and at 10 m are related by:

$$U_{2m} = U_{10m} + \frac{u_*}{k} * \left\{ \ln\left(\frac{2}{10}\right) - \Psi\left(\frac{2}{L}\right) + \left(\frac{10}{L}\right) \right\} \quad (10)$$

where u_*, k and L ($= (u_*^2 \theta)/(\kappa g \theta_*)$) are the friction velocity, the von Karman constant (0.4) and the Obukhov-length, respectively. Ψ corresponds to the integrated flux-profile relationship for the stable surface layer and equals $\Psi = -6(z/L)$.

[37] 4. To make the distinction between rain and snow, a threshold-temperature is normally used [e.g., *Greuell and Konzelmann*, 1994; *Loth et al.*, 1993; *Rowe et al.*, 1995]. However, according to *Loth et al.* [1993], the most serious problem remaining in snow modeling is the choice of a satisfactory criterion to distinguish between snowfall and rain. To overcome the difficulty of estimating the phase of precipitation, it was estimated from the synoptic measurements. Total 6-hourly precipitation is uniformly distributed over the preceding 6 hours.

[38] Figure 4 shows the daily averaged 1990 atmospheric parameters that are used to force the snow-ice model.

3.1.3. Reference and Albedo Sensitivity Experiment

[39] In this section, two experiments will be presented and compared with in-situ snow and ice measurements for the summer of 1990. The experiments differ from each other in the way their snow albedo is parameterized in the integrated surface albedo model.

[40] In the reference experiment, the snow albedo is calculated with the CROCUS snow albedo parameterizations (see equations (2), (3) and (4)). In the albedo sensitivity experiment, the snow albedo is determined using the albedo-surface snow density relationship of *Greuell and Konzelmann* [1994] but without the cloudiness dependency. In this formulation, a fresh snow layer has a prescribed density of 300 kg m^{-3} and the snow albedo is calculated with the following formulation (no solar zenith angle dependency):

$$\alpha = \alpha_{ice} + \left(\rho_{surface} - \rho_{ice}\right)\left[\frac{\alpha_{snow} - \alpha_{ice}}{\rho_{snow} - \rho_{ice}}\right] \quad (11)$$

where $\rho_{surface}$ equals the density of the top layer in the snow model and with $\alpha_{ice} = 0.58$, $\rho_{ice} = 920$ kg m^{-3}, $\alpha_{snow} = 0.85$ and $\rho_{snow} = 300$ kg m^{-3}.

[41] At ETH Camp, the observed variation of the snow albedo is principally due to (1) rapid grain growth in wet snow (large grains lower the albedo), (2) the presence of liquid water which increases the effective snow grain size and (3) the sintering of melting snow grains [*Colbeck*, 1997]. With the albedo-surface snow density parameterization, these effects are represented by the density of the surface snow layer.

[42] The 1990 ablation season has previously been studied and reported in the literature by both *Rowe et al.* [1995] and *Greuell and Konzelmann* [1994] who used similar models although important differences between their models and the model used here exist. The most important differences lie in the treatment of the surface albedo and the drainage of meltwater.

[43] *Greuell and Konzelmann* [1994] used a surface snow density dependent albedo while *Rowe et al.* [1995] prescribed the measured surface albedo. In our case it is calculated from the simulated surface snow grain characteristics.

[44] Free drainage of meltwater is used by *Rowe et al.* [1995] while *Greuell and Konzelmann* [1994] prescribed a slush layer, which in their model is not allowed to drain until it has reached its capacity of 20 cm. In the present study, the use of the runoff parameterization allows a slow drainage of meltwater.

3.1.3.1. The 1990 Reference Experiment

[45] The simulated snow pack height evolution in the reference experiment agrees very well with the observed one (see Figure 5 and Table 2). It can be seen that the modeled date at which the snow disappears coincides closely with the observations, i.e., around day 48.

[46] Contrary to the snow pack height, the observed mass balance is not directly measured. It is calculated from the measured snow pack density, snow pack height, superimposed ice thickness (with a density of 900 kg m^{-3}) and slush thickness (with a density of 950 kg m^{-3}) as explained by *Ohmura et al.* [1992].

[47] In Figure 6 it can be seen that the simulated mass balance lags the observed one. *Greuell and Konzelmann* [1994] found the same. It can be explained by the presence of ice lenses and vertical drainage channels (pipes) which accelerate runoff and which are not taken into account in the model. The final simulated mass balance is overestimated by 8 cm w.e. which consists mainly (i.e., 5.5 cm w.e.) of superimposed ice upon the old ice. In the model, meltwater reaching the bottom of the snow pack is drained away according the runoff algorithm. This takes some time and meanwhile part of the meltwater refreezes upon the old ice as superimposed ice. In reality, almost no superimposed
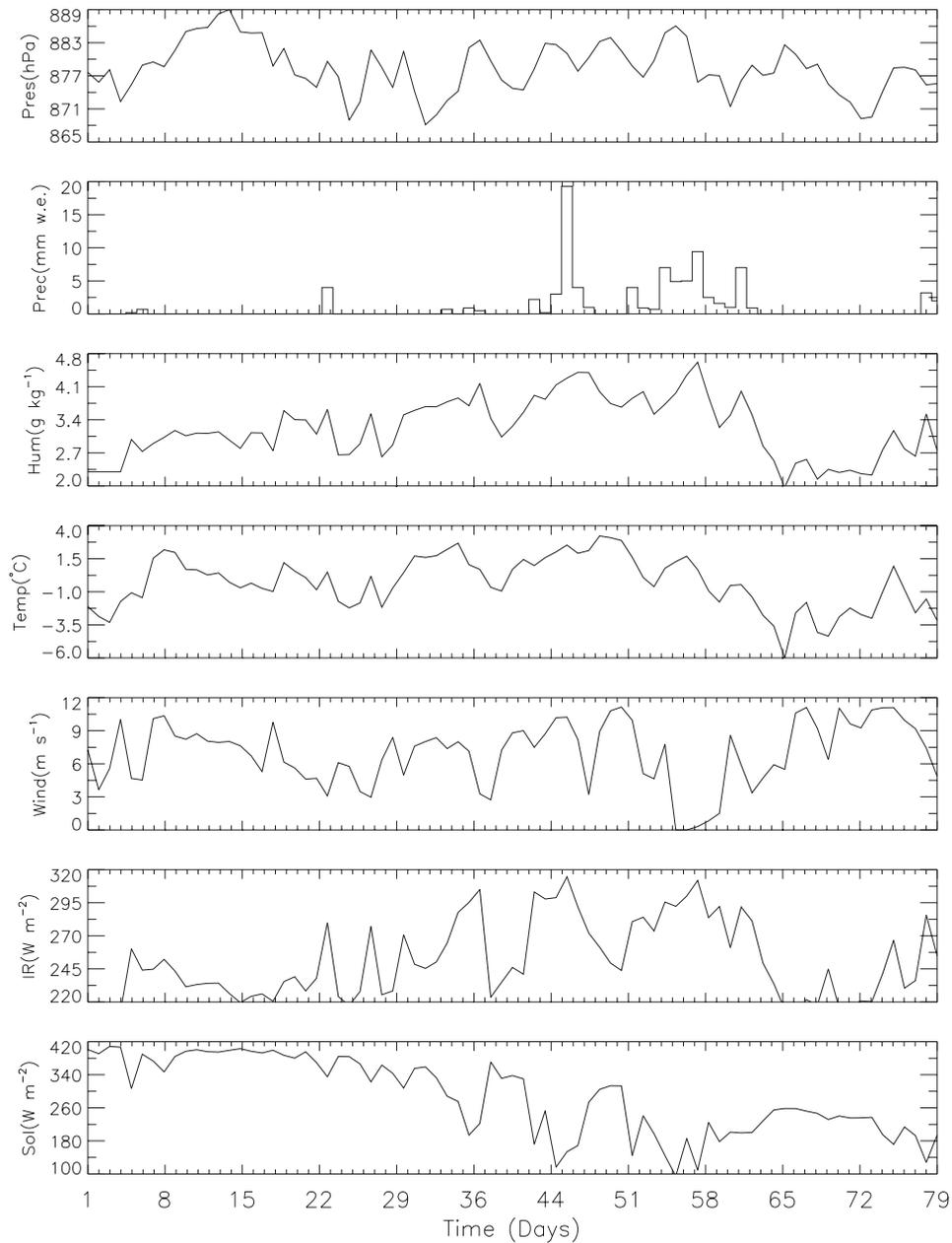
Figure 4. Meteorological conditions at ETH Camp during the 1990 simulation (12 June–29 August). Daily average values are plotted.

ice was observed (estimates range between 2 and 6 cm w.e.), because meltwater was able to percolate and to refreeze in the upper layers of the underlying ice which consisted of porous old ice. This increased the ice temperature and limited further superimposed ice formation [*Ohmura et al.*, 1991]. This porous ice is not represented in the snow model which explains why the superimposed ice formation is overestimated. In their study, *Rowe et al.* [1995] encountered an excessive modeled superimposed ice formation (20 cm w.e.). This was caused by the free drainage of excessive meltwater that was not able to accumulate. Accumulation of meltwater limits the refreezing of meltwater.

[48] The modeled surface albedo is in good agreement with the data (see Figure 7 and Table 2). In both the model

and the data, the surface albedo remained almost constant during the first 30 days of the simulation. Also the important albedo decrease at day 45 is correctly simulated by the model. The observed increase in surface albedo on day 69 is thought to be caused by a small snowfall although the precipitation data show no rain -or snowfall event (Figure 4). This points to a possible error in the albedo data or in the precipitation data on day 69.

[49] Two more figures demonstrate the model's ability to correctly simulate the internal snow pack processes and temporal variability. The simulated and observed mean snow pack density (Figure 8) and liquid water content (Figure 9) are in good agreement with the observations. The observed rapid density increase and wetting of the snow pack between day 5 and day 13 are well resolved by
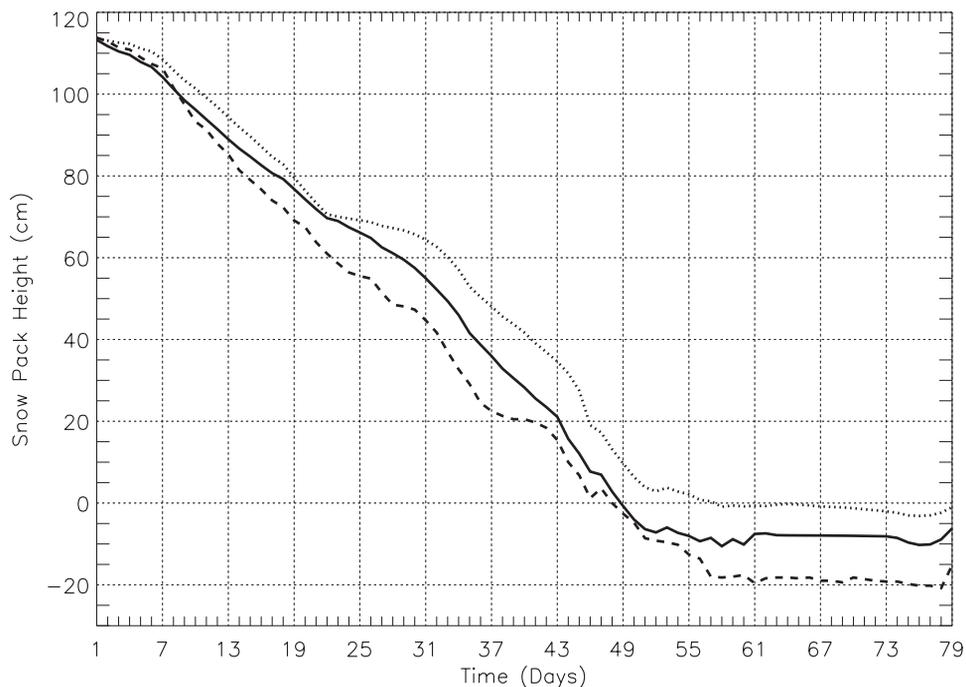
Figure 5. The simulated snow pack height in the 1990 reference (solid line) experiment, in the albedo sensitivity (dotted line) experiment and observations (dashed line). Height is relative to the height of the surface on day 48 when ice appeared at the surface for the first time in the observations.

the model. The modeled overestimated snow pack density between day 26 and day 34 is due to the models shortcoming in determining the slush layers to be excluded and needs further investigation. When calculating the average snow pack density and liquid water content, the model slush layers must be excluded from the snow pack in order to compare the modeled snow pack density with the observations because observed values only refer to the snow pack without the slush layers.

[50] The RMSE of the simulated surface temperature for the whole duration of the simulation equals 1.3°C (see Table 2). Between day 30 and day 59, the snow pack is continuously melting. During the last 20 days of the simulation, melt almost stops, and the surface temperature drops below 0°C. The comparison between the modeled and observed surface temperature evolution during the last 20 days of the reference simulation is shown on Figure 10. It can be seen that the daily temperature cycle is well resolved.

[51] Since the short and long wave incident fluxes as well as rain and snowfall are taken from observations, the surface temperature evolution mainly depends on the quality of the simulated surface albedo, the upward longwave radiative flux as well as the sensible and latent heat fluxes. *Greuell and Konzelmann* [1994] studied the surface energy balance components during the 1990 summer months at ETH Camp. Table 3 compares the surface energy fluxes from both modeling studies. Sensible and latent heat fluxes almost balance each other in both studies which is a common feature for a site close to the equilibrium site [*Box*, 2001]. The common value of 307 Wm^{-2} for the outgoing longwave radiation flux equals the observed value reported by *Konzelmann* [1994]. The difference in total energy for heating and melting of the snow and ice pack

between the two studies is solely due to the difference in surface albedo.

3.1.3.2. The 1990 Albedo Sensitivity Experiment

[52] When a surface snow density dependent snow albedo is used in the integrated albedo model (see equation (11)), the greatest differences with the reference experiment can be seen in the simulation of the surface albedo (Figure 7). The observed, almost constant, snow albedo during the first 30 days, cannot be captured with a surface snow density dependent snow albedo. Consequently, the modeled mass balance deviates largely from the observed one during this period (Figure 6). The modeled underestimation of the snow albedo between day 15 and day 22 is due to an excessively high simulated surface snow density caused by daytime melting and nighttime refreezing of the liquid water content in the surface layers. Indeed, data show that the air temperature fluctuated around 0°C in this period. This melt-

Table 2. Root-Mean-Square Errors (RMSE) of the 1990 and 1991 Simulation for the Reference (CROCUS-α) and the Albedo Sensitivity Experiment (Density-α)

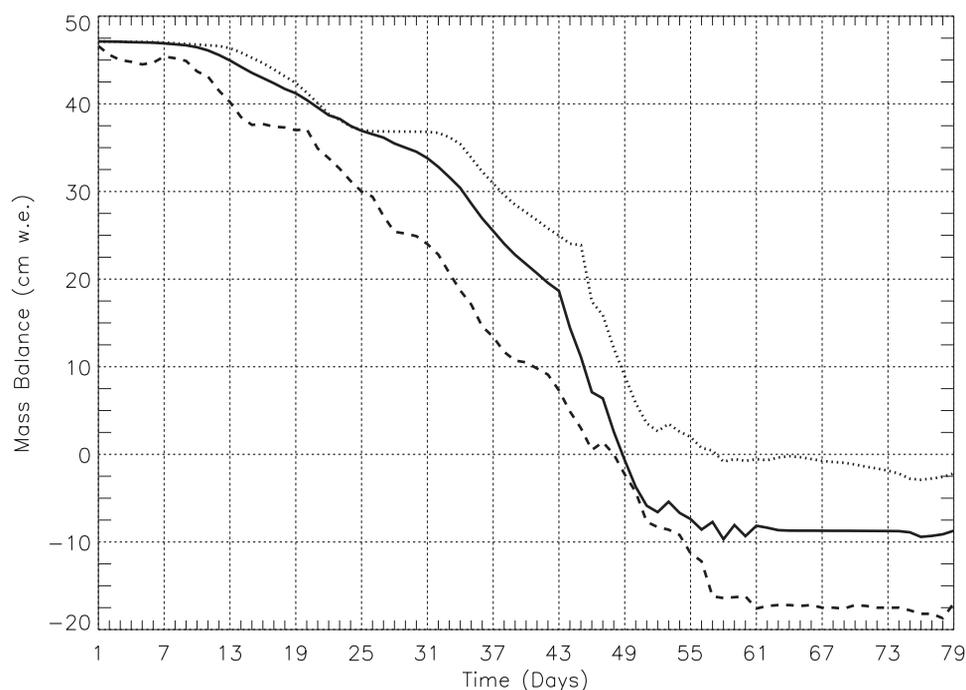|	1990		1991	
	CROCUS-α	Density-α	CROCUS-α	Density-α
Surface albedo RMSE, -	0.04	0.10	0.04	0.05
Surface height RMSE, cm	8.9	16.4	3.5	2.5
Mass balance RMSE, cm w.e.	7.8	13.2	11.2	10.7
Surface temperature RMSE, °C	1.3	1.3	1.3	1.3

Figure 6. As in Figure 5, but for the mass balance.

refreezing cycle caused an increase of the uppermost snow layer density up to 750 kg m^{-3}. *Greuell and Konzelmann* [1994] stated that they solved this problem by using an unrealistically low value for the irreducible water amount (0.02) in order to reduce the densification rate due to refreezing of capillary water. However, they did not compare their modeled average snow pack density and liquid water content with the observations.

[53] A snowfall on day 23 induces an overestimated increase of the albedo. The modeled albedo remains too high until day 32 because there was almost no melt between day 23 and day 32, and hence no important increase in surface snow density.

[54] The snowfall event on day 59 creates a too small increase in surface albedo by the model compared to the observations because the tiny snow layer upon the ice melts
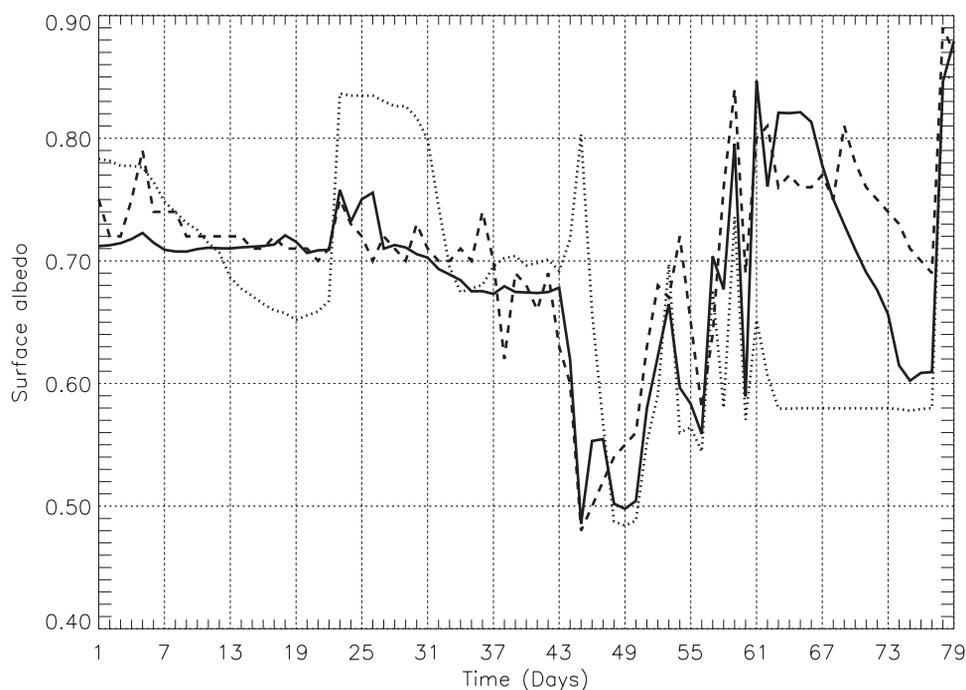

Figure 7. The simulated surface albedo in the 1990 reference experiment (solid line) and the albedo sensitivity experiment (dotted line) compared with observations (dashed line).
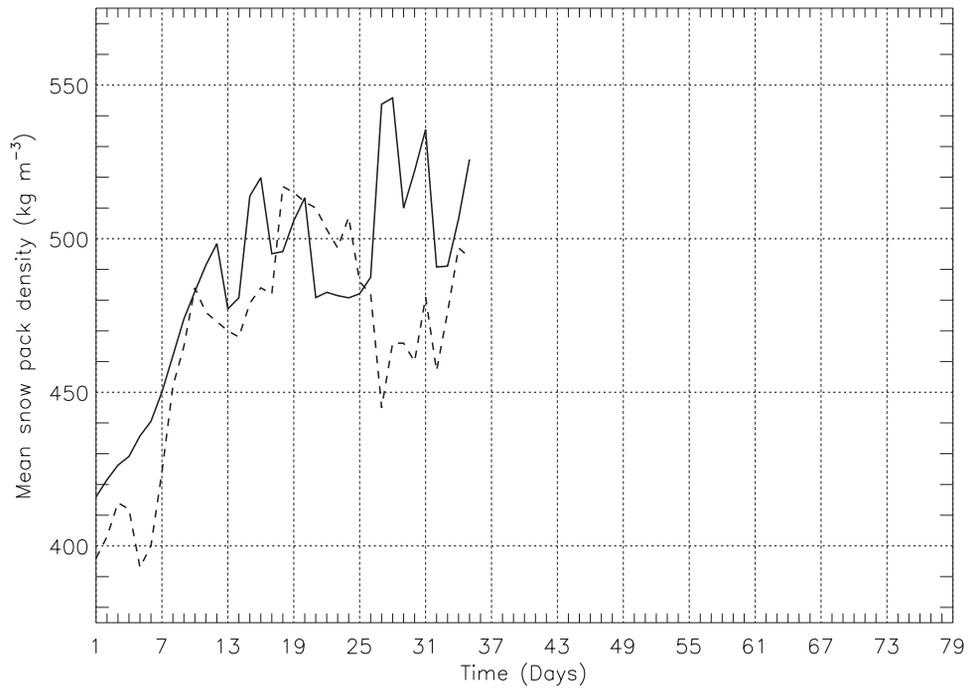
Figure 8. The simulated mean snow pack density in the 1990 reference experiment (solid line) compared with observations (dashed line). Density observations stopped after day 35.

away too quickly. As in the reference experiment, the possible error in the forcing precipitation data on day 69 prevents an albedo increase. Therefore the modeled albedo stays constant between day 63 and day 77 and because the modeled snow pack had disappeared, it equals the ice albedo.

[55] At the end of the density dependent simulation, too much superimposed ice has been formed (13 cm w.e.) compared to the reference experiment (5.5 cm w.e.). This is principally due to the delayed large albedo decrease, and the subsequent underestimated melt of superimposed ice in
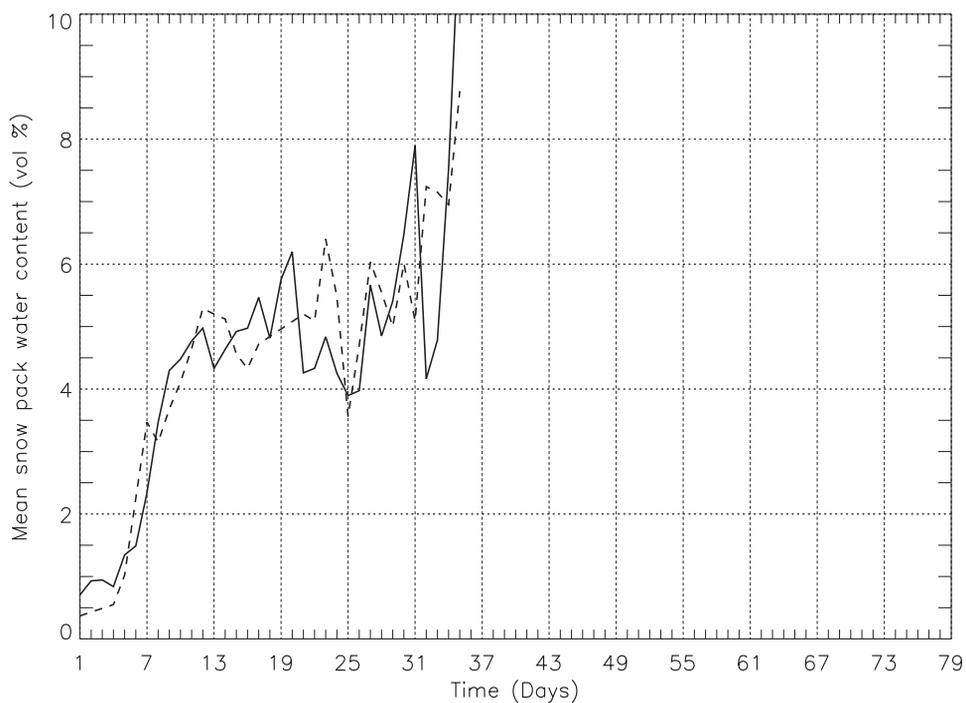

Figure 9. As in Figure 8, but for the mean liquid water content. Liquid water content observations stopped after day 35.
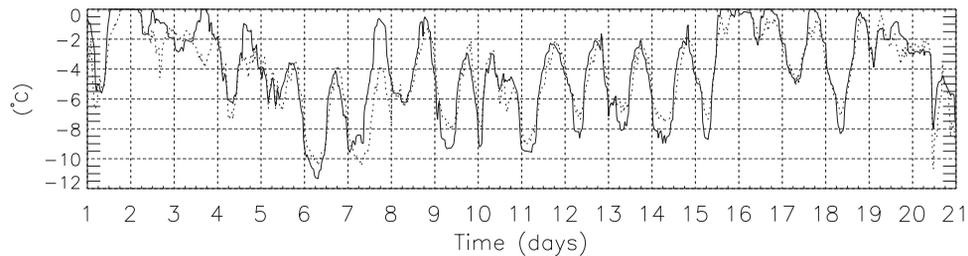
Figure 10. The simulated surface temperature (solid line) compared with observations (dashed line) during the last 20 days of the 1990 reference simulation.

the model, around day 45. The modeled snow pack disappears too late.

3.2. Case 2: Summer of 1991
3.2.1. Initialization of the Snow-Ice Model
[56] The initialization of the snow-ice model for the 1991 experiments is made in a similar way as for 1990. Snow and ice measurements from the 3rd of June 1991 have been used. As for 1990, no layered snow grain size data or snow density and liquid water content data are available. Therefore, the average observed values as well as the observed temperature profile are used to initialize the model. The initial average density for the 1.63 m thick snow pack equals 421 kg m^{-3} and the top 30 cm of the snow pack is temperate with a liquid water content of 1.68 volume %. The snow grains of the wet and dry snow have been set equal to 1.0 and 0.3 mm large spherical snow grains, respectively. 0.3 mm is the smallest possible descriptive grain size for spherical nondendritic snow grains in the model. The grain sizes used to initialize the snow pack are smaller than those that were used to initialize the snow pack in 1990 because almost no melt occurred before the start of the 1991 simulation on June 3rd 1991. At the beginning of the melt season in 1991, almost no ice lenses were observed inside the snow pack [*Konzelmann*, 1994].
3.2.2. Atmospheric Forcing Data
[57] The preparation of the 1991 simulation forcing data (3rd of June until the 18th of August inclusive, i.e., 77 days, see Figure 11) is similar to the procedure followed for the 1990 simulation. 2 days of long wave incoming radiation, 5 days of wind speed, 1 day of temperature and 1 day of specific humidity missing data had to be replaced using linear interpolation. Precipitation consisted of 50 mm w.e.

of rain and 31 mm w.e. of snow, which created a high inter-daily variability in the snow albedo.
3.2.3. Reference and Albedo Sensitivity Experiment
[58] The reference and albedo sensitivity experiments are made with the same model configurations as for the 1990 experiments.
3.2.3.1. The 1991 Reference Experiment
[59] The comparison between the modeled snow pack height and the observations shows a very good agreement (Figure 12). The different rates of decrease of height throughout the melting season are well reproduced. The first period (day 1 until day 14) is characterized by a slow rate of decrease. The following three weeks (day 15 until day 34 with melt on every day, only disturbed by some precipitation events) are marked by a greater decrease rate. Between day 35 and day 50, the surface height lowers at a high constant rate. The model is able to reproduce this feature. On day 71, the surface height starts to rise again indicating the end of the ablation season.
[60] The comparison between the modeled and observed mass balance (Figure 13) needs some attention. The measured increase in mass balance (nearly 10 cm w.e.) during the first 24 days cannot be due to precipitation as only 1 cm w.e. of precipitation was measured. Probably, side-wards inflow of meltwater increased the measured mass balance which of course cannot be captured by the one-dimensional model which supposes horizontal homogeneity. This explains the large discrepancy at day 24 which remains until the end of the simulation. However, the agreement between the total amount of modeled and observed ablation is good.
[61] Figure 14 shows that the CROCUS parameterizations are able to capture adequately the observed albedo variations during the whole 1991 simulation. During the

Table 3. Surface Energy Balance for the Summer of 1990 and 1991[a]

	1990 Experiments of *Greuell and Konzelmann* [1994]	1990 Reference Experiment	1991 Reference Experiment
Period	1/06 – 31/08/1990	12/06 – 29/08/1990	03/06 – 18/08/1991
Global incident rad.	292	287	299
Reflected solar rad.	210	198	230
Absorbed solar rad.	82	89	69
Long wave incident rad.	253	251	262
Long wave upward rad.	307	307	308
Net radiative flux	28	33	23
Sensible heat	34	29	21
Latent heat	−28	−21	−15
Total energy	34	41	29

[a]Fluxes are in W m^{-2}, and the turbulent fluxes are positive downwards. Note that the 1990 values of *Greuell and Konzelmann* [1994] refer to the period "June – July – August."
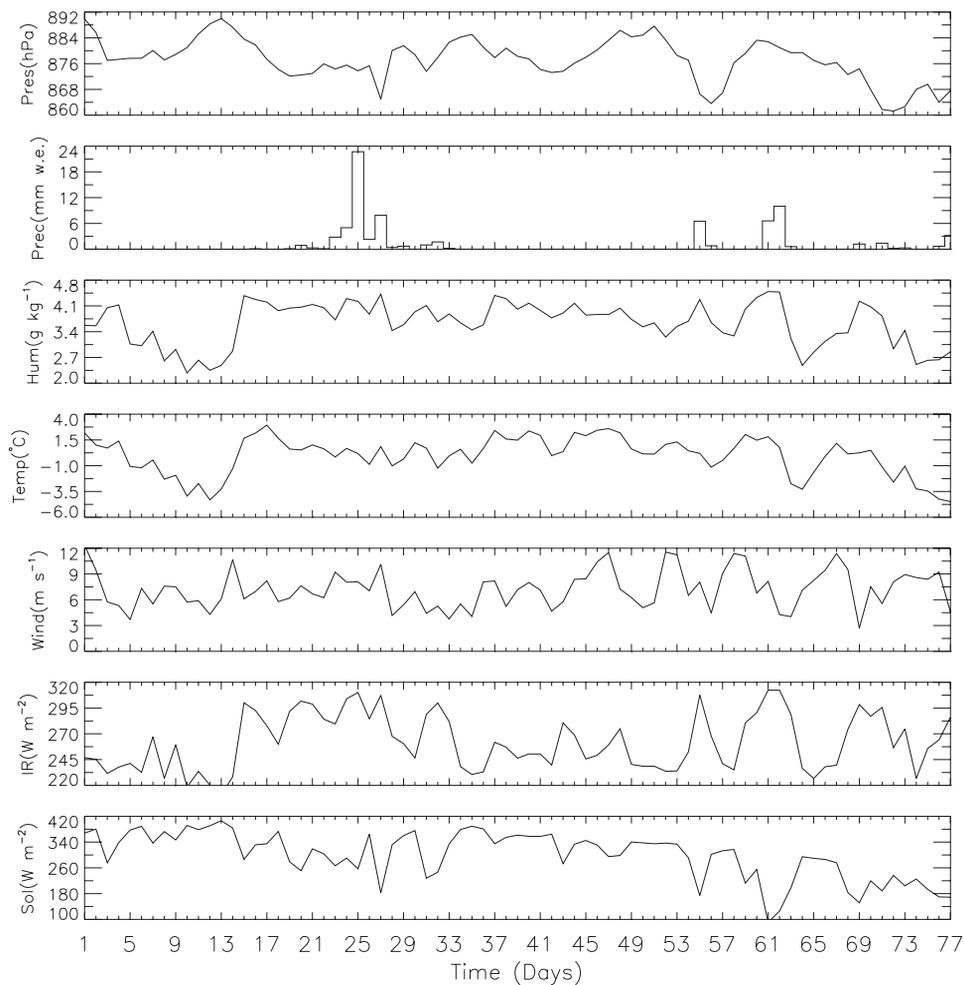
Figure 11. Meteorological conditions at ETH Camp during the 1991 simulation (3 June–18 August). Daily average values are plotted.

first 18 days, no snowfalls occur and the observed albedo decreases to a value of 0.73. The modeled, but not observed, rise of the albedo between day 9 and day 14 can be explained by the modeled formation of almost faceted crystals from rounded crystals without increasing the descriptive grain size. In CROCUS, the descriptive grain size for dry snow is not allowed to increase before the snow crystals are completely faceted. This formation of almost faceted crystals leads to smaller optical grain sizes which explains the rise of the modeled albedo between day 9 and day 14. The modeled formation of faceted crystals in dry snow occurs in the presence of high temperature gradients (see Figure 11). These high temperature gradients are due to low air temperatures and were also observed experimentally. *Dang et al.* [1997] also noticed that CROCUS allows faceted crystal formation in high density dry snow, although this is not verified experimentally. Between day 19 and 33, the observed albedo variations due to frequent snowfall events are well simulated. Afterwards, between day 34 and day 55, the snow pack was continuously melting and the measured albedo rapidly lowered to a value of 0.72 which is well simulated by the model. Between day 55 and day 71, the observed and simulated albedo vary between the albedo of fresh dendritic snow and the albedo of older nondendritic

larger snow grains. These variations (rate and amplitude) are correctly represented in the snow model. After the snowfall on day 71, the modeled albedo decreases too rapidly between day 74 and day 75 because the dry fresh snow rapidly evolves from dendritic snow grains (dendricity = 0.5 and sphericity = 0.5) towards nondendritic fully faceted snow grains (sphericity = 0.0 and descriptive grain size = 0.4 mm). Once the stage of fully faceted crystals is arrived at, they rapidly increase their descriptive grain size which explains why the modeled albedo decreases to 0.75 on day 75. This modeled strong increase of grain size for fully faceted snow grains is based on the functions of *Marbouty* [1980], and occurs in the presence of large temperature gradients. Indeed, between day 74 and day 76, the modeled surface layer cools to $-12°C$ during the night (not shown) which creates a large temperature gradient. This discrepancy between observed and modeled albedo should be investigated in the future.

[62] The root-mean-square error between the simulated and the observed surface temperature is calculated for the whole simulation and for three time periods (days 1–33; days 34–54; days 55–77). Values of 1.3°C, 1.3°C, 1.0°C and 1.6°C, respectively, are obtained. The low value of 1.0°C for the second period can be explained by the almost
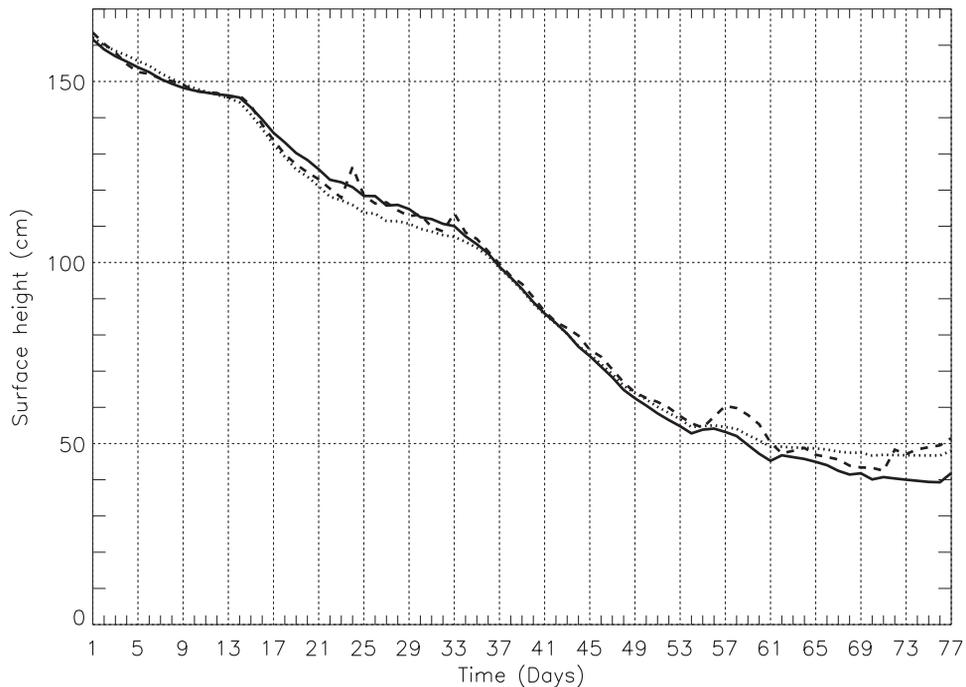
Figure 12. The simulated snow pack height in the 1991 reference (solid line) experiment, in the albedo sensitivity (dotted line) experiment and observations (dashed line). Height is relative to the snow-ice interface at the beginning of the mass-balance measurements.

continuous melting (only during the night does surface temperature drop below zero) of the snow pack. The modeled average surface energy balance fluxes are similar to those during the 1990 melt season (see Table 3).

3.2.3.2. The 1991 Albedo Sensitivity Experiment

[63] In the sensitivity experiment with the surface density dependent snow albedo, the snow pack height (Figure 12) and mass balance (Figure 13) are well reproduced. The
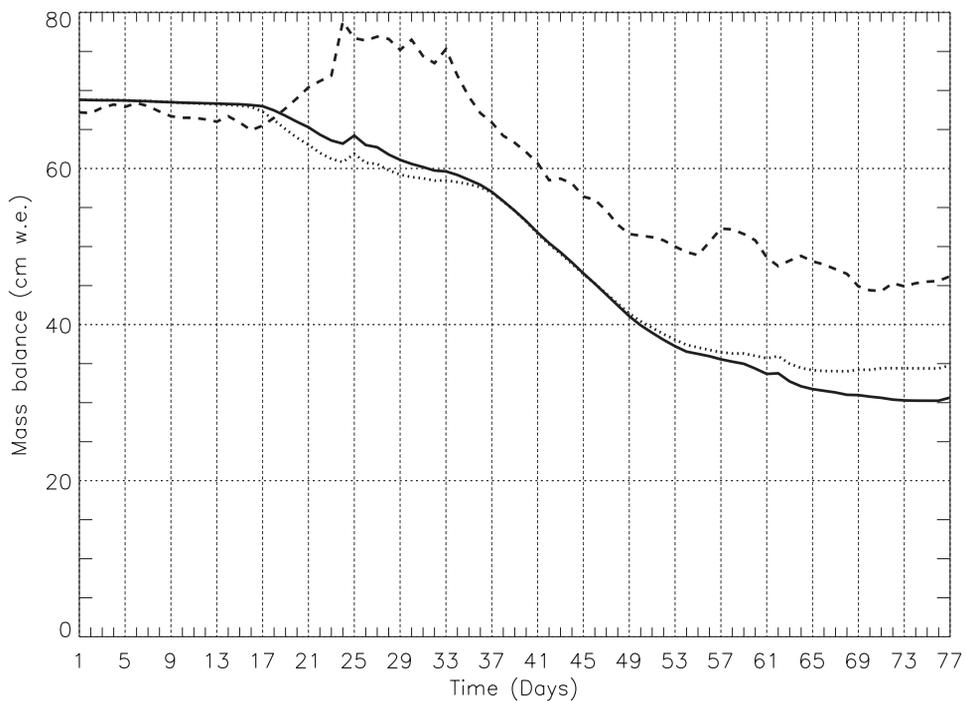

Figure 13. As in Figure 12, but for the mass balance. The difference between the between the measured and modeled mass balance at the end of the simulation mainly originates between day 18 and day 24. A possible explanation is proposed in the mass balance description part of the 1991 reference experiment section.
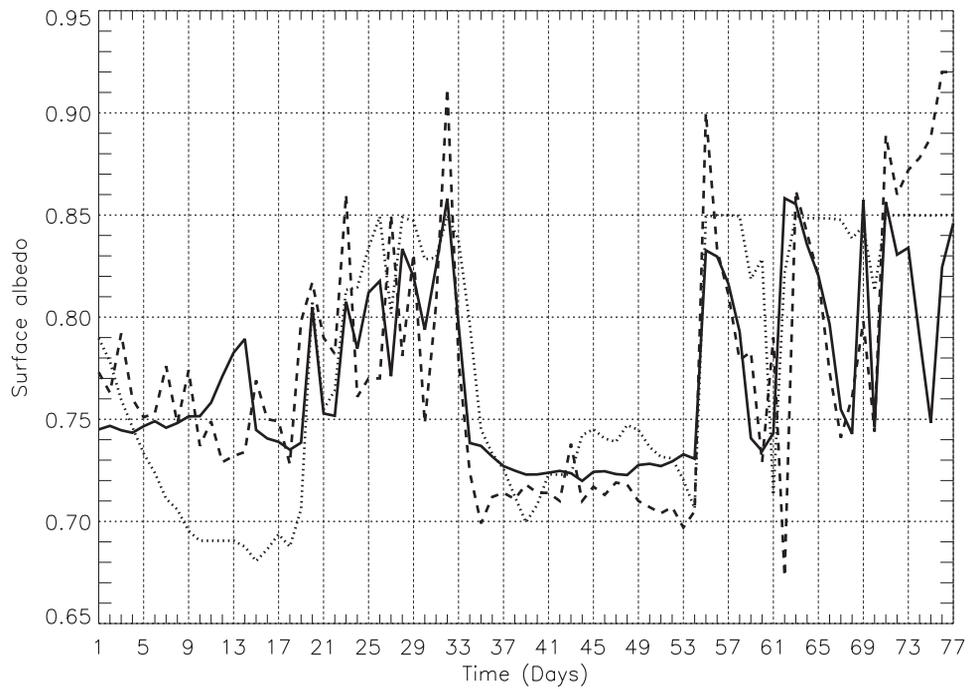
Figure 14. The simulated surface albedo in the 1991 reference experiment (solid line) and the albedo sensitivity experiment (dotted line) compared with observations (dashed line).

results do not differ greatly from the reference experiment (see Table 2) although the simulation of the albedo is somewhat worse than in the reference experiment (Figure 14). With the density dependent snow albedo, the modeled snow pack melting during the first 9 days lowers the simulated snow albedo too much. Afterwards the simulated albedo remains somewhat too high until the beginning of the main melting period (between day 33 and day 55). During the last part of the simulation, the modeled density dependent snow albedo stays constant at 0.85 because the
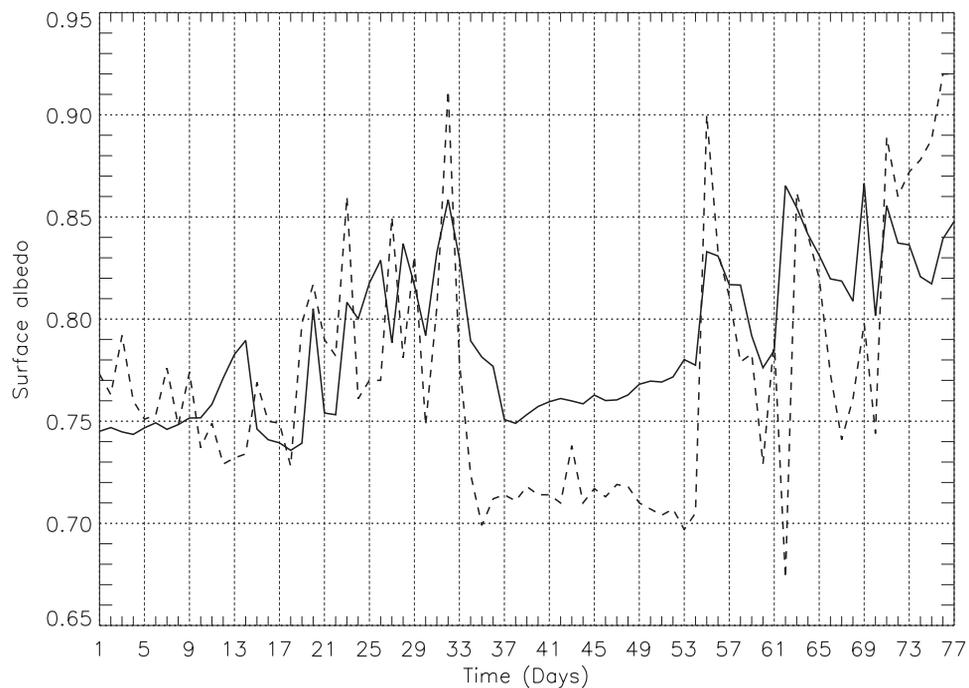

Figure 15. Comparison of the modeled albedo (solid line) in the sensitivity experiment in which the drainage of meltwater in saturation was instantaneous with the measured albedo (dashed line) during the 1991 ablation season.

modeled surface density did not change anymore since almost no more melt took place.

4. Summary and Conclusion

[64] The snow-ice model of the regional atmospheric climate model MAR has been used to simulate snow and ice melting at ETH Camp (West Greenland, 1155 m asl) during the summers of 1990 and 1991 in order to validate the introduction of the CROCUS snow model snow metamorphism and snow albedo parameterizations [*Brun et al.*, 1992]. This has been done because the updated MAR snow model needed to be validated for a polar site on Greenland.

[65] For each summer season, two experiments have been presented. The numerical experiments differ from each other in the way the snow albedo is parameterized in the integrated surface albedo model. In the reference experiment, the CROCUS snow albedo parameterizations are used to calculate snow albedo, while in the albedo sensitivity experiment, snow albedo is calculated from the surface snow density as done by *Greuell and Konzelmann* [1994] but without the cloudiness dependency.

[66] The simulations are compared with observations of snow pack height, mass balance, surface temperature, surface albedo as well as mean snow pack density and liquid water content. A single model configuration was able to provide good results for both the 1990 and 1991 ablation seasons. The simulated surface height is in good agreement with the observations and the simulated mass balance captures the general character of the observations.

[67] The correctly simulated snow albedo points to an appropriate simulation of the surface snow characteristics by the CROCUS snow metamorphism parameterizations for a snow pack upon an almost impermeable ice surface characterized by a small surface slope where meltwater can accumulate and slush layers can be formed. It is necessary to parameterize correctly the runoff of meltwater because of the interaction between the simulated temperature and liquid water content and the simulated snow albedo via the simulated snow grain characteristics. For example, a sensitivity experiment for the 1991 ablation season (see Figure 15) in which abundant meltwater was drained away instantaneously gives rise to higher simulated snow albedo values. The average albedo value increased from 0.77 up to 0.79.

[68] In conclusion, the integrated albedo model with the CROCUS snow albedo allows an adequate representation of the variable snow albedo. Some discrepancies between the observed and modeled albedo have been found for faceted crystals in the presence of a large temperature gradient and for high-density dry snow and these should be investigated in the future.

[69] The use of a simpler density dependent snow albedo also gives satisfactory results but there is a likely compensation of errors during the simulation. For example, when air temperature fluctuates around zero degrees Celsius, refreezing of meltwater during the night causes a too high surface snow density which leads to too low snow albedo values. *Greuell and Konzelmann* [1994] mentioned that they solved this problem by using an unrealistically low value for the irreducible water amount (0.02) in order to reduce the densification rate due to refreezing of capillary water. When air temperature is above zero degrees Celsius, ablation is somewhat underestimated because of a delayed albedo lowering at the beginning of the major melting period. This can be seen for both summers (Figures 7 and 14). The density of the surface snow is a more slowly varying parameter than the surface snow grains morphological characteristics.

[70] This snow-ice model is now ready to be used over Greenland coupled with the regional atmospheric climate model MAR. However it must be noted that some limitations still remain. The spatial and temporal variability of the underlying ice albedo is governed by macro-physical processes (dust transport, meltwater drainage systems, presence of Wisconsin/Holocene ice [*Bøggild et al.*, 1996]) that are not represented in the snow-ice model. The albedo of the ice underlying the seasonal snow pack must therefore be prescribed. Also, in the Greenland percolation zone, ice lenses are commonly found inside the snow and firn cover [*Koerner and Fisher*, 1990; *Pfeffer and Humphrey*, 1996; *Marsh and Woo*, 1984]. At the moment, they are only poorly represented inside the MAR snow model and should be made permeable in the future. Nevertheless, the variable new albedo scheme allows a more accurate simulation of the surface albedo, which is one of the most important parameters in snow melt calculations and which opens new perspectives in the study of the Greenland surface mass balance.

References

Andreas, E., A theory for the scalar roughness and the scalar transfer coefficients over snow and sea ice, *Boundary Layer Meteorol.*, *38*, 159–184, 1987.

Benson, C. S., Stratigraphic studies in the snow and firn of the Greenland ice sheet, *CRREL Res. Rep. 70*, 93 pp., Cold Reg. Res. and Eng. Lab., Hannover, N. H., 1962.

Bøggild, C. E., H. Oerter, and T. Tukiainen, Increased ablation of Wisconsin ice in eastern north Greenland: Observations and modelling, *Ann. Glaciol.*, *23*, 144–148, 1996.

Box, J. E., Surface water vapor exchanges on the Greenland ice sheet derived from automatic weather station data, Ph.D. thesis, Univ. of Colo., Boulder, 2001.

Brun, E., Investigation on wet-snow metamorphism in respect of liquid-water content, *Ann. Glaciol.*, *13*, 22–26, 1989.

Brun, E., P. David, M. Sudul, and G. Brunot, A numerical model to simulate snowcover stratigraphy for operational avalanche forecasting, *J. Glaciol.*, *38*, 13–22, 1992.

Businger, J., Turbulent transfer in the atmospheric surface layer, paper presented at Workshop on Micrometeorology, Am. Meteorol. Soc., Denver, Colo., 1973.

Colbeck, S. C., A theory of water percolation in snow, *J. Glaciol.*, *11*, 369–385, 1972.

Colbeck, S. C., The capillary effects on water percolation in homogeneous snow, *J. Glaciol.*, *13*, 85–97, 1974.

Colbeck, S. C., A review of sintering in seasonal snow, *CRREL Rep. 97-10*, Cold Reg. Res. and Eng. Lab., Hannover, N. H., 1997.

Coléou, C., and B. Lesaffre, Irreducible water saturation in snow: Experimental results in a cold laboratory, *Ann. Glaciol.*, *26*, 64–68, 1998.

Coulson, K., *Solar and Terrestrial Radiation: Methods and Measurements*, Acadamic, San Diego, Calif., 1975.

Dang, H., C. Genthon, and E. Martin, Numerical modelling of snow cover over polar ice sheets, *Ann. Glaciol.*, *25*, 170–176, 1997.

Deardorff, J., Efficient prediction of ground surface temperature and moisture with inclusion of a layer of vegetation, *J. Geophys. Res.*, *83*, 1889–1903, 1978.

Denoth, A., W. Seidenbusch, M. Blumthaler, W. Kirchlechner, W. Ambach, and S. Colbeck, Study of water drainage from columns of snow, *CRREL Rep. 79-1*, Cold Reg. Res. and Eng. Lab., Hannover, N. H., 1979.

Gallée, H., Simulation of the mesocyclonic activity in the Ross Sea, Antarctica, *Mon. Weather Rev.*, *123*, 2051–2069, 1995.

Gallée, H., and P. Duynkerke, Air-snow interactions and the surface energy and mass balance over the melting zone of West Greenland during GIMEX, *J. Geophys. Res.*, *102*, 13,813–13,824, 1997.

Gallée, H., O. Fontaine de Ghélin, and M. R. van den Broeke, Simulation of atmospheric circulation during the GIMEX 91 experiment using a meso-γ primitive equations model, *J. Clim.*, *8*, 2843–2859, 1995.

Gallée, H., G. Guyomarc'h, and E. Brun, Impact of the snow drift on the Antarctic ice sheet surface mass balance: A sensitivity study to snow, *Boundary Layer Meteorol.*, *99*, 1–19, 2001.

Greuell, W., and T. Konzelmann, Numerical modelling of the energy balance and the englacial temperature of the Greenland ice sheet: Calculations for the ETH-Camp location (West Greenland, 1155 m a.s.l.), *Global Planet. Change*, *9*, 91–114, 1994.

Houghton, J., Y. Ding, D. Griggs, M. Noguer, P. van der Linden, X. Dai, K. Maskell, and C. Johnson (Eds.), *Climate Change 2001: The Scientific Basis, Contributions of Working Group I to the Third Assessment Report of the Intergovernmental Panel on Climate Change*, 881 pp., Cambridge Univ. Press, New York, 2001.

Koerner, R., and D. Fisher, A record of Holocene summer climate from a Canadian high-Arctic ice core, *Nature*, *343*, 630–631, 1990.

Konzelmann, T., Radiation conditions on the Greenland ice sheet, *Züricher Geogr. Schr. 56*, ETH Geogr. Inst., Zürich, 1994.

Loth, B., H.-F. Graf, and J. M. Oberhuber, Snow cover model for global climate simulations, *J. Geophys. Res.*, *98*, 10,451–10,464, 1993.

Male, D., The seasonal snowcover, in *Dynamics of Snow and Ice Masses*, edited by S. C. Colbeck, chap. 6, pp. 305–395, Acadamic, San Diego, Calif., 1980.

Marbaix, P., A regional atmospheric model over Europe: Adaptation for climate studies and validation, Ph.D. thesis, Univ. cath. de Louvain, Louvain-la-Neuve, Belgium, 2000.

Marbouty, D., An experimental study of temperature-gradient metamorphism, *J. Glaciol.*, *26*, 303–312, 1980.

Marsh, P., and M.-K. Woo, Wetting front advance and freezing of meltwater within a snow cover: 1. Observations in the Canadian Arctic, *Water Resour. Res.*, *20*, 1853–1864, 1984.

Monin, A., and A. Obukhov, Basic regularity in turbulent mixing in the surface layer of the atmosphere, *Akad. Nauk SSSR Tr. Geofiz. Inst.*, no. *24*, 163–187, 1954.

Munro, D., Surface roughness and bulk heat transfer on a glacier: Comparison with eddy correlation, *J. Glaciol.*, *35*, 343–348, 1989.

Oerlemans, J., and H. Vugts, A meteorological experiment in the melting zone of the Greenland Ice Sheet, *Bull. Am. Meteorol. Soc.*, *74*, 355–365, 1993.

Ohmura, A., K. Steffen, H. Blatter, W. Greuell, M. Rotach, T. Konzelmann, M. Laternser, A. Ouchi, and D. Steiger, Energy and mass balance during the melt season at the equilibrium line atlitude, Paakitsoq, Greenland ice sheet, *Prog. Rep. 1*, Dep. of Geogr., Swiss Fed. Inst. of Technol., Zürich, 1991.

Ohmura, A., et al., Energy and mass balance during the melt season at the equilibrium line atlitude, Paakitsoq, Greenland ice sheet: *Prog. Rep. 2*, Dep. of Geogr., Swiss Fed. Inst. of Technol., Zürich, 1992.

Pfeffer, W., and N. Humphrey, Determination of timing and location of water movement and ice layer formation by temperature measurements in sub-freezing snow, *J. Glaciol.*, *42*, 292–304, 1996.

Randall, D., et al., Analysis of snow feedback in 14 general circulation models, *J. Geophys. Res.*, *99*, 20,757–20,771, 1994.

Rowe, C. M., K. C. Kuivinen, and R. Jordan, Simulation of summer snowmelt on the Greenland ice sheet using a one-dimensional model, *J. Geophys. Res.*, *100*, 16,265–16,273, 1995.

Segal, M., J. Garratt, R. Pielke, and Z. Ye, Scaling and numerical model evaluation of snow-cover effects on the generation and modification of daytime mesoscale circulations, *J. Atmos. Sci.*, *48*, 1024–1042, 1991.

Smeets, C., P. Duynkerke, and H. Vugts, Observed wind profiles and turbulence fluxes over an ice surface with changing surface roughness, *Boundary Layer Meteorol.*, *92*, 101–123, 1999.

Wiscombe, W. J., and S. G. Warren, A model for the spectral albedo of snow. i: Pure snow, *J. Atmos. Sci.*, *37*, 2712–2733, 1980.

Zuo, Z., and J. Oerlemans, Modelling albedo and specific balance of the Greenland ice sheet: Calculations for the Søndre Strømfjord transect, *J. Glaciol.*, *42*, 305–317, 1996.

———————————

H. Gallée, Laboratoire de Glaciologie et Géophysique de l'Environnement, 54 rue Molière, BP 96, F-38402 Saint-Martin d'Hères Cedex, France. (gallee@glaciog.ujf-grenoble.fr)

W. Greuell, Institute for Marine and Atmospheric Research, Utrecht University, Princetonplein 5, NL-3584 Utrecht, Netherlands. (w.greuell@phys.uu.nl)

F. Lefebre, VITO-TAP, Boeretang 200, B-2400 Mol, Belgium. (filip.lefebre@vito.be)

J.-P. van Ypersele, Institut d'Astronomie et de Géophysique G. Lemaître, Université catholique de Louvain, 2 Chemin du Cyclotron, B-1348 Louvain-la-Neuve, Belgium. (vanypersele@astr.ucl.ac.be)